Retinoic acid signaling within pancreatic endocrine progenitors regulates mouse and human β cell specification

David S. Lorberbaum[1], Siddharth Kishore[2,3], Carolina Rosselot[4], Dylan Sarbaugh[1], Elliott P. Brooks[1], Eloise Aragon[1], Shouhong Xuan[5], Olivier Simon[6], Debashis Ghosh[6], Cathy Mendelsohn[7], Paul Gadue[2,3], Lori Sussel[1,8,*]

[1]Barbara Davis Center for Diabetes, University of Colorado Anschutz Medical Campus, Aurora, CO, USA.
[2]Center for Cellular and Molecular Therapeutics, The Children's Hospital of Philadelphia, Philadelphia, PA, USA; Department of Pathology and Laboratory Medicine, The Children's Hospital of Philadelphia, Philadelphia, PA, USA
[3]Department of Cell and Molecular Biology, Perelman School of Medicine, University of Pennsylvania, Philadelphia, PA, USA
[4]Division of Endocrinology, Diabetes and Bone Diseases, Diabetes, Obesity and Metabolism Institute, Icahn School of Medicine at Mount Sinai, New York, NY, USA
[5]Department of Medicine Hematology and Oncology, Columbia University Medical Center, New York, USA
[6]Department of Biostatistics and Informatics, Colorado School of Public Health University of Colorado Anschutz Medical Campus, Aurora, CO, USA
[7]Department of Urology, Columbia University, New York, NY, USA
[8]Lead contact

*Author for correspondence: lori.sussel@ucdenver.edu

Key Words

β cell differentiation, retinoic acid signaling, WNT signaling, pancreas development, diabetes, δ cell specification

Summary Statement

Retinoic acid signaling regulates pancreatic β cell differentiation in mice and humans and represses δ cell gene expression during islet specification via WNT signaling.

Abstract

Retinoic acid (RA) signaling is essential for multiple developmental processes, including appropriate pancreas formation from the foregut endoderm. RA is also required to generate pancreatic progenitors from human pluripotent stem cells. However, the role of RA signaling during endocrine specification has not been fully explored. In this study, we demonstrate that disruption of RA signaling within the NEUROG3-expressing endocrine progenitor population impairs mouse β cell differentiation and induces ectopic expression of critical δ cell genes, including *Somatostatin*. In addition, inhibition of the RA pathway in hESC-derived pancreatic progenitors downstream of NEUROG3 induction impairs INSULIN expression. We further determine that RA-regulation of endocrine cell differentiation is mediated through WNT pathway components. Together, these data demonstrate the importance of RA signaling in endocrine specification and identify conserved mechanisms by which RA signaling directs pancreatic endocrine cell fate.

Introduction

Cell signaling pathways are used continuously throughout development and adulthood to mediate tissue interactions and precisely control gene expression. In particular, retinoic acid (RA) signaling plays critical roles in a wide range of developmental processes at multiple stages during embryogenesis (Ghyselinck and Duester, 2019). In vertebrates, the basic mechanisms of RA function are conserved: Vitamin A is converted into RA through a series of enzymatic reactions and enters the nucleus to interact with the transcriptional effectors of the pathway, RAR and RXR, as well as co-activators and co-repressors to regulate context specific target genes (Fig. S1A).

In the pancreas, RA signaling is necessary for the onset of pancreagenesis; previous studies have demonstrated that inhibition of this pathway leads to pancreas agenesis (Arregi et al., 2016, Oström et al., 2008, Molotkov et al., 2005, Martín et al., 2005, Stafford and Prince, 2002). Based on these studies, exogenous RA is included in human pluripotent stem cell (hPSC) β-like cell differentiation protocols to facilitate the earliest stages of pancreas development. While high levels of RA are crucial for initial pancreas specification, RA has been shown to subsequently inhibit endocrine differentiation in several model systems (Cardenas-Diaz et al., 2019, Pagliuca et al., 2014, Huang et al., 2014, Rezania et al., 2012, Rovira et al., 2011), therefore most protocols use progressively lower doses of RA after pancreatic endoderm specification. Despite the reduction or exclusion of exogenous sources of RA from endocrine differentiation media at these later differentiation stages, it has been shown that a cell-autonomous source of RA may still exist (Huang et al., 2014). This is also supported by gene expression analyses in mice demonstrating the presence of many key RA pathway genes in the embryonic pancreas (Krentz et al., 2018). The function of RA signaling during vertebrate islet endocrine cell differentiation, however, has not been fully explored.

To define the role of RA signaling during pancreas endocrine development, we inhibited RA signaling specifically in endocrine progenitors by expressing the *RARdn* under the regulation of the *Neurog3:cre* allele. These studies demonstrated that RA signaling is required for both β cell specification and inhibition of δ cell gene

transcripts, including *Hhex, Rbp4,* and *Somatostatin*. Inhibition of RA in the NEUROG3^{+} endocrine progenitor population resulted in reduced numbers of insulin-producing β cells, and contributed to impaired blood glucose regulation in postnatal and adult mice. Similarly, chemical inhibition of RA specifically after NEUROG3 induction in hPSC β-like cell differentiations decreased *INSULIN* production. At the molecular level, we demonstrate that RA-mediated repression of WNT signaling allows for proper endocrine cell differentiation. Together, these results establish the importance of RA signaling in the endocrine progenitor population for appropriate mouse and human β cell specification.

Results and Discussion

The RARdn efficiently disrupts pancreas development in mice

To disrupt RA signaling in a cell-specific manner, we used the previously described dominant negative human retinoic acid receptor allele that had been inserted into the *R26R* locus downstream of a flox-stop-flox cassette (*RARdn^{flox}*; Fig. S1B; (Rosselot et al., 2010)). To validate that the *RARdn* allele functioned appropriately, we generated *RARdn$^{flox/flox}$*; *Pdx1:Cre* mice to broadly inhibit RA signaling in pancreatic progenitors. Similar to previous studies (Oström et al., 2008), disruption of RA signaling in all pancreatic progenitors led to the formation of a smaller pancreas that contained fewer β (INSULIN, or INS), α (GLUCAGON, or GCG), and δ cells (SOMATOSTATIN, or SST) at e16.5 and e18.5 (Fig. S1C). Disrupting RA signaling using the tamoxifen-inducible *Pdx1:creEsr1* allele (Gu et al., 2002) at e9.5, a slightly later stage of development after the pancreatic progenitor population has been established, also resulted in the formation of a smaller pancreas and a significant reduction in islet cluster formation and fewer hormone producing cells (Fig. S1D-G).

Endocrine specific RA inhibition impairs the formation of insulin-producing β cells and causes ectopic Somatostatin RNA expression

To determine whether RA signaling was also required during endocrine cell differentiation downstream of endocrine progenitor formation, we disrupted RA signaling specifically within the NEUROG3 endocrine progenitor population using *RARdn$^{flox/flox}$*; *Neurog3:cre* mice. Remarkably, disrupting RA signaling in the

endocrine progenitor population resulted in significantly fewer β cells as early as e16.5, without notable changes in the other endocrine cell types (Fig. 1A-B). The timing of reduced β cell numbers, combined with no apparent changes in β cell death or proliferation, suggests inhibition of RA signaling in endocrine progenitor cells impairs β cell differentiation (Fig. 1C,D).

Consistent with the reduced number of β cells in the *RARdn*$^{flox/flox}$; *Neurog3:cre* mice, there was also a reduction of *Ins1* and *Ins2* RNA expression (Fig. 1E). Interestingly, however, there was also a significant increase in *Sst* RNA that did not correspond to an increase in δ cell numbers (Fig. 1E compared to Fig. 1B). To determine the explanation for discordant expression between *Sst* RNA and δ cell numbers, we performed RNA-scope combined with immunofluorescence on e16.5 pancreatic tissue sections. This analysis verified an increase in cells expressing *Sst* RNA, many of which were not SST protein-producing δ cells (Fig. 1F-G, arrows). *Sst* transcripts could be detected in other endocrine cell types, including INSULIN-producing β cells, but not in GLUCAGON-producing α cells (Fig. 1G, yellow arrows and data not shown). We also observed an additional class of *Sst*+ cells that do not co-express INS, SST, or GCG (Fig. 1G, white arrows and data not shown), which could represent a population of β cells that no longer express INS. However, the observed percentage of *Sst*+/SST^{-} cells does not correlate with the more substantial decrease in β cell numbers in RA mutants (Fig. 1B and 1F), suggesting the β cell loss is at least partially independent of the upregulation of the δ cell transcriptional program.

Postnatal hormone expression and blood glucose homeostasis are disrupted in RA mutants

To determine whether the endocrine cell defects persisted postnatally, we assessed hormone expression in postnatal day 2 (p2) mice. Consistent with the defects observed at e16.5, the reduction in the number of INS+ β cells and *Ins* transcript was maintained in neonates and was again accompanied by an increase in *Sst* RNA expression without an impact on δ cell numbers (Fig. 2A-C). Furthermore, the *RARdn*$^{flox/flox}$; *Neurog3:cre* neonatal mice were overtly hyperglycemic compared to littermate *Neurog3:cre* controls (Fig. 2D). Although there was a significant reduction

in β cell numbers, the observed decrease is not usually sufficient to cause hyperglycemia (Bonner-Weir et al., 1983, Yasugi et al., 1976), suggesting that the remaining β cells in *RARdn*$^{flox/flox}$; *Neurog3:cre* mice are dysfunctional, which could at least partially be explained by the ectopic expression of δ cell transcripts within the INS+ β cell population. This is also consistent with the glucose intolerance phenotype observed when RA signaling was specifically inhibited in adult mouse β cells (Brun et al., 2015). *RARdn*$^{flox/flox}$; *Neurog3:cre* mice had a normal lifespan, however impaired glucose homeostasis persisted into adulthood (Fig. 2E-F).

RA signaling regulates human β cell differentiation after pancreas progenitor specification

To determine whether the role of RA signaling in murine pancreatic endocrine specification was conserved during human β cell differentiation, we inhibited RA signaling at stage 4 (PP1, day 11) of the human β cell differentiation protocol (Fig. 3A) (Cardenas-Diaz et al., 2019, Tiyaboonchai et al., 2017). Differentiation of human pluripotent stem cells (hPSCs) into β-like cells requires the addition of RA from stages 1 through 2 (days 3-8) to generate PDX1 expressing posterior foregut-like cells; as well as between stages 2 and 5 (days 8-13), during which time *NEUROG3* begins to be expressed (Fig. 3A-B). To simulate our murine *in vivo* experiments, we inhibited RA signaling after NEUROG3 induction by excluding exogenous RA from the media starting at stage 4 (PP1, day 11) and adding the high affinity pan-RAR inhibitor, AGN193108, to the culture media (RAi, Fig. 3A-B) (Johnson et al., 1999). To ensure we had not altered pancreatic progenitor differentiation, we confirmed the presence of PDX1/NKX6.1 double positive cells at day 13, two days after treatment with RAi (Fig. 3C). Following 2 additional weeks of culture in RAi supplemented media to inhibit any potential role of autocrine RA signaling during endocrine specification, we observed a significant decrease in *INS* RNA, with no statistically significant changes in either *GCG* or *SST* RNA expression (Fig. 3D). Analysis of endocrine cell numbers at day 28 showed there was also a decrease in C-PEPTIDE+ cells, although this did not reach significance. These findings are in contrast to a report by Huang et al. that demonstrated RA inhibition in human endocrine cell differentiation led to increased INS, GCG, and SST (Huang et al.,

2014). These differences may be due to the method of RA inhibition, as Huang and colleagues employed an ALDH inhibitor that acts upstream of RAR and does not inhibit all ALDH enzymes, allowing the possibility that RA signaling could continue via other ALDH homologs (Morgan et al., 2015, Duester, 2001). Inhibition of the RA pathway at the RAR/RXR level effectively avoids potential compensatory mechanisms that could reduce the efficacy of upstream inhibitors. Overall, our results suggest that in humans, RA signaling is important for achieving optimal *INS* production, and to a lesser extent, β cell differentiation (Fig. 3D,G compared to Fig. 2A-B and 1B,E).

WNT signaling is derepressed in RARdn$^{flox/flox}$; Neurog3:cre mutants during murine endocrine specification

To identify pathways regulated by RA signaling in the endocrine progenitor lineage, we performed transcriptome analysis of whole mouse pancreata at e16.5 and found 1392 significantly changed genes (padj ≤ 0.05) in *RARdn$^{flox/flox}$*; *Neurog3:cre* mutant mice, including *Ins1, Ins2,* and *Sst* (Fig. 4A-B, Table S1). In addition to the increase in *Sst* transcript, we also identified several other upregulated δ cell genes, including *Hhex*, *Rbp4*, and *Crhr2* (Fig. 4C) (DiGruccio et al., 2016), suggesting RA signaling in endocrine progenitors is necessary to repress ectopic expression of the δ cell transcriptional program. Although there were also changes in several RA associated genes, classic RA targets such as *HoxA1 (Marshall et al., 1996)* and *Cyp26A1 (Loudig et al., 2000)* that have been described in other developmental contexts were not significantly altered (Fig. 4A-B, Table S1). This is likely due to the absence of these genes in the NEUROG3+ endocrine progenitor population (Krentz et al., 2018), and demonstrates that RA targets are highly context dependent. Interestingly, we did observe a modest reduction (pval=0.057, padj = 0.253) in *Mnx1*, a known RA-regulated pancreatic development factor (Dalgin et al., 2011). Endocrine deletion of *Mnx1* resulted in reduced β cells and increased δ and α cells (Pan et al., 2015). Although we did not observe an α cell phenotype in *RARdn$^{flox/flox}$*; *Neurog3:cre* mutants, this may be due to the lesser reduction of *Mnx1* expression.

To better define the molecular mechanisms by which RA signaling in the murine endocrine lineage affects the development of hormone producing cells, we completed a gene ontology (GO) term analysis (Mi et al., 2019) of significantly changed genes at e16.5. These GO terms revealed that WNT signaling components were significantly affected by inhibition of RA (Fig. 4D), including 9 WNT associated genes that were all upregulated (Fig. 4E). Bioinformatic analysis identified putative RARα binding sites in the promoter elements of two of these WNT associated genes, *Smo* and *Ror1,* suggesting they may be directly regulated by RA signaling (Table S2). The identification of tissue specific enhancers will be necessary to uncover a direct link between RA and the remaining dysregulated WNT signaling components, which will likely involve both direct and indirect regulation by RA and/or WNT pathway components. As expected, this analysis also identified RARα binding sites in the promoter-proximal regions of several dysregulated RA associated genes including *Muc4*, *Aldh1b1*, and *Ret*, validating the analysis. The dysregulated δ cell genes, however, were not enriched for RARα binding sites in their promoter regions, however, there are several developmental studies indicating *Hhex* is indirectly regulated by Wnt/β-Catenin (Rankin et al., 2011, McLin et al., 2007).

The upregulation of WNT pathway components by RA inhibition reveals that under normal conditions RA functions to repress WNT signaling – directly and/or indirectly - to promote appropriate β cell differentiation and inhibit δ cell gene transcription (Fig. 4F). This RA-WNT interaction has been shown to be an important mediator of development in several other biological contexts (Kumar and Duester, 2010), (Bonney et al., 2018, Bonney et al., 2016), (Osei-Sarfo and Gudas, 2014), (Roa et al., 2019) and importantly is consistent with recent studies suggesting that inhibition of endogenous WNT is necessary for improved stem cell-derived β cell maturation in human cells (Vethe et al., 2019, Sharon et al., 2019). Our findings suggest that the addition of RA, even in small amounts, to the human β cell differentiation protocol during endocrine progenitor specification could inhibit WNT signaling to promote more robust generation of β cells and that RA-mediated WNT repression is necessary to repress δ cell genes in non-δ endocrine cells. Interestingly, we did not observe an increase in *SST* transcript expression in the human β cell differentiation platform. This could be due to the fact that the *in vitro* hPSC model has been

engineered to optimally generate β cells, rather than the other endocrine cell fates. Alternatively, the unperturbed human *SST* RNA levels could suggest that disruption of β cell differentiation and upregulation of the δ cell transcriptional program are separable events, as indicated by the lack of direct correlation between the two phenotypes in the *RARdn*$^{flox/flox}$; *Neurog3:cre* mutants (Fig. 1B,1F-G), with only the RA regulation of β cell differentiation being conserved in humans. Finally, it is remains possible that this discrepancy between mice and humans could be attributed to the artificial nature of the *in vitro* β cell differentiation system.

The ability to generate β cells *in vitro* from hPSCs has greatly improved during the last decade; however, despite significant progress, direct differentiation of functionally mature human β cells in culture remains a challenge. Since these differentiation protocols have been extensively informed by developmental studies in rodent models, we examined RA signaling, a critical mediator of early pancreas formation, in the differentiation of pancreatic endocrine cells in both mice and in the differentiation of human β-like cells. Inhibiting the RA pathway in NEUROG3+ mouse and human pancreatic endocrine progenitors resulted in defective β cell production and *Ins* expression, phenotypes that are at least partially due to derepression of the WNT signaling pathway. This study also identified a novel role for RA signaling for repression of δ cell gene expression. Taken together, these data demonstrate a conserved, previously unappreciated role of RA signaling during pancreatic endocrine development. These results will inform β cell differentiation conditions to facilitate the generation of functionally mature human β cells *in vitro* and advancing our understanding of pancreatic endocrine development.

Materials and Methods

Animal Models

Mice were maintained under protocol 00045 as approved by the University of Colorado Denver Institutional Animal Care and Use Committee (IUCUC). All animals were bred on a mixed C57Bl6/129SV genetic background and group housed by sex of up to 5 siblings in each cage with constant access to food and water at room

temperature, 22°C. Cages were changed once every two weeks and regularly monitored for virus and parasite infection, which were never present during this study. Euthanasia was performed by CO_2 inhalation and by cervical dislocation after asphyxiation as a secondary method of euthanasia. For timed matings, the identification of a vaginal plug in the morning was defined as embryonic day 0.5. The male was removed from the cage and the female was monitored to ensure pregnancy until sacrifice. All mice and embryos were genotyped with primers listed in Table S4 using standard PCR with Go Taq DNA Polymerase Mastermix (Promega). All mice used are available from Jackson Laboratories: Tg(Neurog3-cre)C1Able/J (Cat# 005667; RRID:IMSR_JAX:005667), B6.FVB-Tg(Pdx1-cre)6Tuv/J (Cat# 014647 RRID:IMSR_JAX:014647); *Gt(ROSA)26Sor*$^{tm1(RARA*)Soc}$/HsvJ (Cat# 029812 RRID:IMSR_JAX:029812); and Tg(Pdx1-cre/Esr1*)#Dam/J (Cat# 024968 RRID:IMSR_JAX:024968).

hPSC culture

All the human pluripotent stem cell (hPSC) studies were performed using the authenticated and routinely checked for contamination H1 human embryonic stem cell (hESCs) line (Thomson et al., 1998). hPSC cell lines were cultured on 0.1% gelatin and irradiated mouse embryonic fibroblast (MEF) feeder cells in DMEM/F12 supplemented with 2mM of glutamine, 15% Knockout Serum Replacement (KSR, 1X NEAA, penicillin/streptomycin, 0.1mM β-mercaptoethanol and 10ng/ml of bFGF. This hPSC medium was changed every day. Cells were passaged when they reach 80% confluence, approximately every 4 days, using TrypLE at a 1:6 ratio. In all hPSC cultures, 5 μM Rho-associated protein kinase (ROCK) inhibitor Y-27632 (Selleck Chemicals, #S1049) was only added into the culture media for ~18 hours when passaging or thawing hPSCs.

Embryoid body generation

hPSCs were incubated with the accutase solution for 7 mins at 37°C, transferred to a 50ml falcon tube and washed twice using 40ml of DMEM-F12. 5.5 million cells were resuspended in 5ml of hPSC medium with 1 μM of ROCK inhibitor and plated in one well of an ultra-low attachment 6-well cell culture plate. The plate was placed on a

100rpm orbital shaker inside a 37°C incubator with 5% CO2. The cells form embryoid bodies overnight and were fed for two days using hPSC medium. After two days, the medium was removed and replaced with pancreatic differentiation medium for day 0.

Pancreatic differentiation from hPSCs

Pancreas differentiation was initiated on the hPSC embryoid bodies with day 0 media containing RPMI supplemented with 3μM Chir99021 and 100μg/ml Activin A. On day 1 media was changed to RPMI with 100μg/ml Activin A, 0.3μM Chir99021 and 5μg/ml bFGF. Day 2 was SFD with 100μg/ml Activin A. From days 3 to 5 cells were fed with DMEM-F12 containing 0.25mM ascorbic acid, 50ng/ml FGF7 and 1.25μM IWP2. Day 6-8 media contained DMEM high glucose (5g/L) supplemented with 1:100 B27 without RA, 1X glutamax, 0.25mM ascorbic acid, 1:200 ITS-X, 50ng/ml FGF7, 0.5μM SANT-1, 1μM Retinoic Acid, 100nM LDN-193189 and 500nM Phorbol. Media for days 9-11 consisted of DMEM high glucose (5g/L) supplemented with 1:100 B27 without RA, 1X glutamax, 0.25mM ascorbic acid, 1:200 ITS-X, 2ng/ml FGF7, 0.5μM SANT-1, 0.1μM Retinoic Acid, 200nM LDN-193189 and 250nM Phorbol. From days 11-13 the media was changed to MCDB131 supplemented with 20mM glucose, 2% FBS, 1X Glutamax, 1:200 ITS-X, 10ug/ml Heparin, 10uM Zinc sulfate, 0.5μM SANT-1, 0.05μM Retinoic Acid, 200nM LDN-193189, 1μM T3 and 10μM ALK5i II. For experiments with the pan-RAR inhibitor, 2μM of AGN193108 was added to the media from day 11 onwards. Cells were harvested on day 13 for flow cytometry analysis and RNA collection using 0.25% Trypsin for 5 minutes. From day 13-28 cells were fed every other day with media that contained MCDB131 with 20mM glucose, 2% FBS, 1X Glutamax, 1:200 ITS-X, 10ug/ml Heparin, 10uM Zinc sulfate, 200nM LDN-193189, 1μM T3, 10μM ALK5i II and 100nM GSIS XX. Cells were harvested on day 28 (β-like stage) for flow cytometry analysis and RNA collection.

Immunofluorescence

Tissues were fixed in 4% paraformaldehyde (PFA) for 4 hours at 4°C, washed in cold 1xPBS, and incubated in 30% sucrose overnight at 4°C. The next day, samples were incubated in 50%OCT (in sucrose) for 15 minutes, 100% OCT for 15 minutes, and

frozen on dry ice. Blocks were sectioned between 10-12uM for immunofluorescence. All antibodies used in this studies are found in Table S3. In brief, samples were blocked in 2% normal donkey serum for 30 minutes, and incubated with primary antibodies overnight at 4°C. The next day, they were washed in PBS-T and incubated in secondary antibodies for 1-3 hours, washed in PBS-T, incubated in DAPI for 10 minutes, washed in PBS-T, and mounted using hard-set Vectashield. For prolonged storage >2 weeks, nail polish was used to seal the edges of coverslip and slides were stored at 4°C. For TUNEL staining, the TMR cell death red kit (Millipore 12156792910) was used per manufacturer's instructions, prior to antibody staining for Insulin.

Morphometric analysis

For protein quantification, the pancreas was completely sectioned and every 10th slide was stained and quantified (5 slides for e16.5 and 10 slides for p2). All e16.5 embryos were sectioned without further dissection of the pancreas. At p2 the pancreas, stomach, duodenum, and intestines were isolated. Images were obtained at 20x magnification using a Leica DM5500B. For both stages, DAPI positive pancreas area was measured and not significantly different between control and mutant samples. At e16.5, individual hormone positive cells were counted manually using FIJI or Adobe Photoshop counting tools. p2 samples were quantified by hormone positive area/DAPI positive area using a Matlab program (available upon request) to detect positively stained pixels in each fluorescent channel. Antibody information can be found in Table S3. All quantification was done blinded to genotype.

RNA extraction and RT-qPCR in mice

Whole pancreata were collected and total RNA extractions were completed using the RNA Easy Mini Kit and eluted in 30ul RNAse-free H_20. 200ng of RNA was used to generate cDNA via the iScript cDNA synthesis kit (Biorad). This cDNA was then diluted in RNAse free H_20 to 1ng/ul, and 4ng cDNA was used in each qPCR reaction using the SsoAdvanced Universal Probes Supermix (Biorad) with Taqman probes (Table S3) and run on the Bio-Rad CFX96 real time PCR detection system. All

expression levels were normalized to *Actb* and quantified using the $2^{-\Delta\Delta Ct}$ method; control samples were averaged and set to one to determine gene expression changes in mutants.

RNA-sequencing

RNA was extracted as described and quality was checked by obtaining RIN values using the Eukaryote Total RNA Nano kit for the Agilent 2100 Bioanalyzer. RIN values for samples >8.0 were subjected to RNA-sequencing using the NovaSEQ 6000 for paired end sequencing (2x150) from PolyA selected total RNA by the University of Colorado Cancer Center Genomics and Microarray Core Facility. Reads were quality checked using FastQC and subjected to Cutadapt to trim adapters. These reads were then aligned to Mm10 using HISAT2 (Kim et al., 2015). Aligned reads were mapped to genes using Ensembl (Mus_musculus.GRCm38.95.gtf) and HTseq-count. Files were converted from SAM to BAM, as well as aligned to the genome using SAMtools (Li et al., 2009). Differential gene expression was examined using the DESeq2 package (Love et al., 2014) in R-studio. Full RNA-seq FastQ files and read counts are available via GEO accession number GSE144953. Gene ontology enrichment analysis was carried out by using Panther (Mi et al., 2019).

Putative RARα binding site identification

Transcript locations and sequences of promoter regions defined as 0-500bp upstream of the TSS for differentially expressed genes were gathered using the GenomicFeatures package in R-studio (Lawrence et al., 2013). These promoter proximal sequences were searched for the JASPER Rara_1 PB0053.1 position weight matrix (PWM) using the Biostrings package in R-studio (https://bioconductor.org/packages/release/bioc/html/Biostrings.html). Only motif matches with a quantitative PWM score that is $\geq$80% of the maximum score were kept for consideration (Wasserman and Sandelin, 2004).

Glucose Tolerance Tests

Mice were fasted overnight (~16 hours) and blood glucose was measured from tail vein blood for a 0min time point just prior to a 2mg D-glucose/gram mouse mass intraperitoneal injection. Blood glucose was monitored at 15, 30, 45, 60, 90, and 120 minutes after injection. All blood glucose measurements were completed using the Contour 7151H blood-glucose monitor with Contour 7097C blood glucose strips.

RNAscope

RNAscope was performed largely as described in ACD biosciences RNAscope Fluorescent Multiplex Kit Quick Guide (https://acdbio.com/documents/product-documents). Already fixed and sectioned e16.5 samples were post fixed at 4°C overnight in 4% PFA. The next morning, slides were washed in DI water and dehydrated using a series of increasing concentrations of ethanol and baked at 60°C for 10 min before being treated with hydrogen peroxide for 10 min. Antigen retrieval was carried out by boiling sections in target retrieval reagent for 10 seconds which were then allowed to cool to RT for 5 minutes. Slides were washed with DI water and subjected to mild protease digestion for 20 minutes in a humified chamber, washed again in DI water and incubated in prewarmed probes (Table S3) for 2 hours at 40°C. Slides were washed with 1x wash buffer and placed in 5x SSC overnight. The next morning, slides were again washed in wash buffer and incubated in AMP1, 2, and 3 solutions for 30min, 30 min, and 15min, respectively, at 40°C, with washes in wash buffer in between each incubation. To develop signal, we used Opal dyes (Table S3) diluted in multiplex TSA buffer for only the channels we visualized in each experiment. Each channel was developed sequentially by incubating samples in HRP-C1/2/3 for 15min at 40°C, washed, and then incubated in the pre-diluted Opal dye for 30min at 40°C. Slides were then washed in wash buffer and incubated in HRP blocker for 15min at 40°C. This solution was removed and slides were again cleaned in wash buffer, then in PBS-T, and subjected to antibody staining as described, but mounted using prolong gold mounting media in place of VectaShield. All samples were imaged at 63x on a Zeiss LSM800 confocal microscope.

Flow Cytometry

Single cell suspensions were prepared by treating cells with 0.25% Trypsin/EDTA for 3 to 5 minutes. For intracellular staining, cells were fixed with 1.6% paraformaldehyde (Electron Microscopy Science) for 30 minutes at 37°C. Cells were washed, permeabilized and stained with 1X saponin buffer (Biolegend). Primary antibodies were diluted to the appropriate concentrations in 100uL of saponin buffer and cells were stained for 30 minutes at room temperature. Samples were washed using 100uL saponin twice and incubated for 30min using the appropriated secondary antibody. Following the staining, cells were resuspended in FACS buffer (DPBS with 0.1% BSA and 0.1% sodium azide). All samples were run on a FACSCantos II or Cytoflex flow cytometer (Becton Dickinson) and analyzed using FlowJo (Treestar) software program.

RNA extraction and RT-qPCR in human cells

Cells were lysed using Lysis buffer provided with the PureLink RNA Micro Kit (Invitrogen Cat No 12183-016) and stored at -80°C. To harvest RNA, samples were thawed out at 4°C and RNA was extracted using the PureLink RNA Micro Kit following the manufacturer's instructions. 14µl of RNAse free water was used to re-suspend the isolated RNA. cDNA was produced using the SuperScript™ III First-Strand Synthesis System kit (Invitrogen). Quantitative PCR was carried out on a LightCycler 480 II with SYBR select master mix (Invitrogen). For all experiments, *TBP* (Veazey and Golding, 2011) was used as a housekeeping gene to determine relative gene expression levels.

Quantification and Statistical Analysis

Graphs and statistical analyses were generated using GraphPad Prism 8. Statistical analyses include n values (biological replicates), statistical test, and significance based on either p-value/p-adjusted value/q-value are detailed in the Fig. legends. For mouse analyses, each n value represents a different animal. Analyses were done with littermate controls, when available. Gender was not assessed for any embryonic studies, but all adult mouse glucose tolerance tests were completed on male mice. The e16.5 RNA-sequencing experiments were analyzed by the DESeq2

platform that reports both p-value and p-adjusted, the latter being used as a significance cutoff at padj $\leq$ 0.05 as defined by the Benjamini-Hochberg procedure, which corrects for multiple hypothesis testing.

Acknowledgments

We thank members of the Sussel lab for helpful feedback on this project, specifically Dr. Michelle Guney and Alexandra Theis for critical readings of the manuscript along with Helen Moses and Amira Sheikh for technical assistance. We also thank Dr. Julie Siegenthaler (University of Colorado Denver) for generously providing us with the *RARdn*^{flox} mice. We are grateful for technical assistance for many specialized techniques and analyses presented here: RNA-sequencing was conducted by the University of Colorado Denver Microarray and Genomics core at the cancer center by Katrina Diener, RNA-sequencing analysis was completed with substantial help from Dr. Ruth Singer and the CU Denver RNA Biosciences Initiative, and RNAscope experiments were assisted by Dr. Laura Hudish.

Competing Interests

The authors declare no competing interests.

Funding

This work was supported by the American Diabetes Association #1-18-PDF-107 (to D.S.L.), National Institutes of Health R01 DK118155 (to P.G. and L.S.), and the National Institutes of Health R01 DK082590 (to L.S.).

Data Availability

Sequencing data are available from GSE144953 in the GEO database. The MatLab program used for analyses of hormone expression at p2 is available upon request.

Author Contributions

Conceptualization, D.S.L., C.R., S.X., L.S.; Methodology, D.S.L., S.K., C.R., S.X., P.G., L.S.; Software; O.S., D.G.; Formal Analysis, D.S.L., D.S., E.B., E.A., S.K.; Investigation; D.S.L., S.K., C.R., D.S., E.B., E.A., S.X.; Resources, O.S. D.G. C.M., P.G., L.S.; Data Curation, D.S.L., O.S., D.G.; Writing – Original Draft, D.S.L. and L.S.; Writing – Review and Editing, D.S.L., S.K., C.R., P.G., L.S.; Visualization: D.S.L., S.K., P.G., L.S.; Supervision, D.G., C.M., P.G., L.S.; Funding Acquisition, D.S.L., P.G., L.S.

References

Arregi, I., Climent, M., Iliev, D., Strasser, J., Gouignard, N., Johansson, J. K., Singh, T., Mazur, M., Semb, H., Artner, I., Minichiello, L. & Pera, E. M. 2016. Retinol Dehydrogenase-10 Regulates Pancreas Organogenesis and Endocrine Cell Differentiation via Paracrine Retinoic Acid Signaling. *Endocrinology,* 157**,** 4615-4631.

Bonner-Weir, S., Trent, D. F. & Weir, G. C. 1983. Partial pancreatectomy in the rat and subsequent defect in glucose-induced insulin release. *J Clin Invest,* 71**,** 1544-53.

Bonney, S., Dennison, B. J. C., Wendlandt, M. & Siegenthaler, J. A. 2018. Retinoic Acid Regulates Endothelial beta-catenin Expression and Pericyte Numbers in the Developing Brain Vasculature. *Front Cell Neurosci,* 12**,** 476.

Bonney, S., Harrison-Uy, S., Mishra, S., Macpherson, A. M., Choe, Y., Li, D., Jaminet, S.-C., Fruttiger, M., Pleasure, S. J. & Siegenthaler, J. A. 2016. Diverse Functions of Retinoic Acid in Brain Vascular Development. *Journal of Neuroscience,* 36**,** 7786-7801.

Brun, P.-J., Grijalva, A., Rausch, R., Watson, E., Yuen, J. J., Das, B. C., Shudo, K., Kagechika, H., Leibel, R. L. & Blaner, W. S. 2015. Retinoic acid receptor signaling is required to maintain glucose-stimulated insulin secretion and β-cell mass. *FASEB journal : official publication of the Federation of American Societies for Experimental Biology,* 29**,** 671-683.

Cardenas-Diaz, F. L., Osorio-Quintero, C., Diaz-Miranda, M. A., Kishore, S., Leavens, K., Jobaliya, C., Stanescu, D., Ortiz-Gonzalez, X., Yoon, C., Chen, C. S., Haliyur, R., Brissova, M., Powers, A. C., French, D. L. & Gadue, P. 2019. Modeling Monogenic Diabetes using Human ESCs Reveals Developmental and Metabolic Deficiencies Caused by Mutations in HNF1A. *Cell Stem Cell,* 25**,** 273-289 e5.

Dalgin, G., Ward, A. B., Hao Le, T., Beattie, C. E., Nechiporuk, A. & Prince, V. E. 2011. Zebrafish mnx1 controls cell fate choice in the developing endocrine pancreas. *Development,* 138**,** 4597-608.

Digruccio, M. R., Mawla, A. M., Donaldson, C. J., Noguchi, G. M., Vaughan, J., Cowing-Zitron, C., Van Der Meulen, T. & Huising, M. O. 2016. Comprehensive alpha, beta and delta cell transcriptomes reveal that ghrelin selectively activates delta cells and promotes somatostatin release from pancreatic islets. *Molecular metabolism,* 5**,** 449-458.

Duester, G. 2001. Genetic dissection of retinoid dehydrogenases. *Chemico-biological interactions,* 130-132**,** 469-480.

Ghyselinck, N. B. & Duester, G. 2019. Retinoic acid signaling pathways. *Development,* 146**,** dev167502.

Gu, G., Dubauskaite, J. & Melton, D. A. 2002. Direct evidence for the pancreatic lineage: NGN3+ cells are islet progenitors and are distinct from duct progenitors. *Development,* 129**,** 2447-57.

Huang, W., Wang, G., Delaspre, F., Vitery Mdel, C., Beer, R. L. & Parsons, M. J. 2014. Retinoic acid plays an evolutionarily conserved and biphasic role in pancreas development. *Dev Biol,* 394**,** 83-93.

Kim, D., Langmead, B. & Salzberg, S. L. 2015. HISAT: a fast spliced aligner with low memory requirements. *Nat Methods,* 12**,** 357-60.

Krentz, N. a. J., Lee, M. Y. Y., Xu, E. E., Sproul, S. L. J., Maslova, A., Sasaki, S. & Lynn, F. C. 2018. Single-Cell Transcriptome Profiling of Mouse and hESC-Derived Pancreatic Progenitors. *Stem cell reports,* 11**,** 1551-1564.

Kumar, S. & Duester, G. 2010. Retinoic acid signaling in perioptic mesenchyme represses Wnt signaling via induction of Pitx2 and Dkk2. *Dev Biol,* 340**,** 67-74.

Lawrence, M., Huber, W., Pages, H., Aboyoun, P., Carlson, M., Gentleman, R., Morgan, M. T. & Carey, V. J. 2013. Software for computing and annotating genomic ranges. *PLoS Comput Biol,* 9**,** e1003118.

Li, H., Handsaker, B., Wysoker, A., Fennell, T., Ruan, J., Homer, N., Marth, G., Abecasis, G., Durbin, R. & Genome Project Data Processing, S. 2009. The Sequence Alignment/Map format and SAMtools. *Bioinformatics,* 25**,** 2078-9.

Loudig, O., Babichuk, C., White, J., Abu-Abed, S., Mueller, C. & Petkovich, M. 2000. Cytochrome P450RAI(CYP26) promoter: a distinct composite retinoic acid response element underlies the complex regulation of retinoic acid metabolism. *Molecular endocrinology (Baltimore, Md.),* 14**,** 1483-1497.

Love, M. I., Huber, W. & Anders, S. 2014. Moderated estimation of fold change and dispersion for RNA-seq data with DESeq2. *Genome Biol,* 15**,** 550.

Marshall, H., Morrison, A., Studer, M., Popperl, H. & Krumlauf, R. 1996. Retinoids and Hox genes. *FASEB J,* 10**,** 969-78.

Martín, M., Gallego-Llamas, J., Ribes, V., Kedinger, M., Niederreither, K., Chambon, P., Dollé, P. & Gradwohl, G. 2005. Dorsal pancreas agenesis in retinoic acid-deficient Raldh2 mutant mice. *Developmental biology,* 284**,** 399-411.

Mclin, V. A., Rankin, S. A. & Zorn, A. M. 2007. Repression of Wnt/beta-catenin signaling in the anterior endoderm is essential for liver and pancreas development. *Development,* 134**,** 2207-2217.

Mi, H., Muruganujan, A., Huang, X., Ebert, D., Mills, C., Guo, X. & Thomas, P. D. 2019. Protocol Update for large-scale genome and gene function analysis with the PANTHER classification system (v.14.0). *Nat Protoc,* 14**,** 703-721.

Molotkov, A., Molotkova, N. & Duester, G. 2005. Retinoic acid generated by Raldh2 in mesoderm is required for mouse dorsal endodermal pancreas development. *Developmental Dynamics,* 232**,** 950-957.

Morgan, C. A., Parajuli, B., Buchman, C. D., Dria, K. & Hurley, T. D. 2015. N,N-diethylaminobenzaldehyde (DEAB) as a substrate and mechanism-based inhibitor for human ALDH isoenzymes. *Chem Biol Interact,* 234**,** 18-28.

Osei-Sarfo, K. & Gudas, L. J. 2014. Retinoic acid suppresses the canonical Wnt signaling pathway in embryonic stem cells and activates the noncanonical Wnt signaling pathway. *Stem Cells,* 32**,** 2061-71.

Oström, M., Loffler, K. A., Edfalk, S., Selander, L., Dahl, U., Ricordi, C., Jeon, J., Correa-Medina, M., Diez, J. & Edlund, H. 2008. Retinoic acid promotes the

generation of pancreatic endocrine progenitor cells and their further differentiation into beta-cells. *PloS one,* 3**,** e2841.

Pagliuca, F. W., Millman, J. R., Gürtler, M., Segel, M., Van Dervort, A., Ryu, J. H., Peterson, Q. P., Greiner, D. & Melton, D. A. 2014. Generation of Functional Human Pancreatic β Cells In Vitro. *Cell,* 159**,** 428-439.

Pan, F. C., Brissova, M., Powers, A. C., Pfaff, S. & Wright, C. V. E. 2015. Inactivating the permanent neonatal diabetes gene Mnx1 switches insulin-producing β-cells to a δ-like fate and reveals a facultative proliferative capacity in aged β-cells. *Development,* 142**,** 3637-3648.

Rankin, S. A., Kormish, J., Kofron, M., Jegga, A. & Zorn, A. M. 2011. A gene regulatory network controlling hhex transcription in the anterior endoderm of the organizer. *Dev Biol,* 351**,** 297-310.

Rezania, A., Bruin, J. E., Riedel, M. J., Mojibian, M., Asadi, A., Xu, J., Gauvin, R., Narayan, K., Karanu, F., O'neil, J. J., Ao, Z., Warnock, G. L. & Kieffer, T. J. 2012. Maturation of human embryonic stem cell-derived pancreatic progenitors into functional islets capable of treating pre-existing diabetes in mice. *Diabetes,* 61**,** 2016-29.

Roa, L. A., Bloemen, M., Carels, C. E. L., Wagener, F. & Von Den Hoff, J. W. 2019. Retinoic acid disrupts osteogenesis in pre-osteoblasts by down-regulating WNT signaling. *Int J Biochem Cell Biol,* 116**,** 105597.

Rosselot, C., Spraggon, L., Chia, I., Batourina, E., Riccio, P., Lu, B., Niederreither, K., Dollé, P., Duester, G., Chambon, P., Costantini, F., Gilbert, T., Molotkov, A. & Mendelsohn, C. 2010. Non-cell-autonomous retinoid signaling is crucial for renal development. *Development,* 137**,** 283-292.

Rovira, M., Huang, W., Yusuff, S., Shim, J. S., Ferrante, A. A., Liu, J. O. & Parsons, M. J. 2011. Chemical screen identifies FDA-approved drugs and target pathways that induce precocious pancreatic endocrine differentiation. *Proc Natl Acad Sci U S A,* 108**,** 19264-9.

Sharon, N., Vanderhooft, J., Straubhaar, J., Mueller, J., Chawla, R., Zhou, Q., Engquist, E. N., Trapnell, C., Gifford, D. K. & Melton, D. A. 2019. Wnt Signaling Separates the Progenitor and Endocrine Compartments during Pancreas Development. *Cell Rep,* 27**,** 2281-2291 e5.

Stafford, D. & Prince, V. E. 2002. Retinoic acid signaling is required for a critical early step in zebrafish pancreatic development. *Current biology : CB,* 12**,** 1215-1220.

Thomson, J. A., Itskovitz-Eldor, J., Shapiro, S. S., Waknitz, M. A., Swiergiel, J. J., Marshall, V. S. & Jones, J. M. 1998. Embryonic stem cell lines derived from human blastocysts. *Science (New York, N.Y.),* 282**,** 1145-1147.

Tiyaboonchai, A., Cardenas-Diaz, F. L., Ying, L., Maguire, J. A., Sim, X., Jobaliya, C., Gagne, A. L., Kishore, S., Stanescu, D. E., Hughes, N., De Leon, D. D., French, D. L. & Gadue, P. 2017. GATA6 Plays an Important Role in the Induction of Human Definitive Endoderm, Development of the Pancreas, and Functionality of Pancreatic beta Cells. *Stem Cell Reports,* 8**,** 589-604.

Vethe, H., Ghila, L., Berle, M., Hoareau, L., Haaland, O. A., Scholz, H., Paulo, J. A., Chera, S. & Raeder, H. 2019. The Effect of Wnt Pathway Modulators on Human iPSC-Derived Pancreatic Beta Cell Maturation. *Front Endocrinol (Lausanne),* 10**,** 293.

Wasserman, W. W. & Sandelin, A. 2004. Applied bioinformatics for the identification of regulatory elements. *Nat Rev Genet,* 5**,** 276-87.

Yasugi, H., Mizumoto, R., Sakurai, H. & Honjo, I. 1976. Changes in carbohydrate metabolism and endocrine function of remnant pancreas after major pancreatic resection. *Am J Surg,* 132**,** 577-80.

Figures

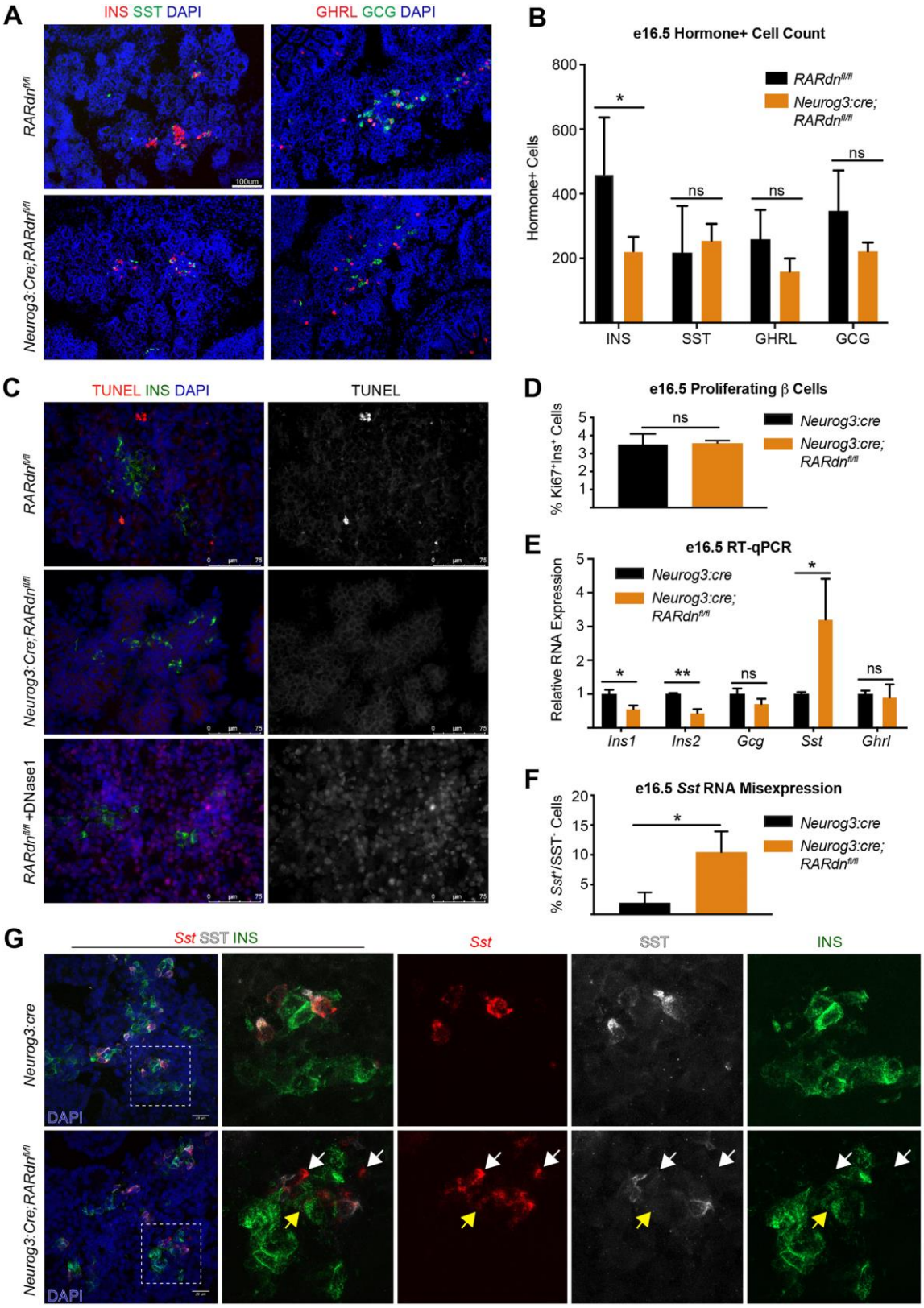

Fig. 1. Endocrine specific RA inhibition disrupts β cell development by e16.5 and increases *Sst* transcript expression. (A) Representative immunofluorescence

images of e16.5 INS, SST, GCG, and GHRL in *RARdn*$^{flox/flox}$*;Neurog3:cre* mutants. (B) Quantification of (A), (n=4 control, n=5 mutant; statistical analysis was completed for multiple t-tests using the Holm-Sidak method to correct for multiple comparisons, padj <0.05* is significant). (C) TUNEL+INS staining at e16.5. DNase1(+) sample is a positive control (n=3) . (D) β cell proliferation reported as a percentage of proliferating vs. non-proliferating β cells (n=3, statistical analysis was completed by an unpaired, parametric t-test, p>0.05, not significant). (E) Gene expression analysis by RT-qPCR of e16.5 whole pancreata from *RARdn*$^{flox/flox}$*;Neurog3:cre* mutants (n=3, statistical analysis was completed by the Benjamini, Krieger, and Yekutieli two-stage step method to correct for multiple comparisons, q values <0.05 *, <0.005** are significant). (F) Quantification of the percentage of cells expressing *Sst* RNA but not SST protein (relative to all *Sst* RNA^{+} cells) in *Neurog3:cre* alone or *RARdn*$^{flox/flox}$*;Neurog3:cre* mutants at e16.5 (n=3, statistical analysis was completed by an unpaired, parametric t-test, p<0.05* is significant). Representative images can be seen in Fig. 1G. (G) Dual RNA-protein visualization using RNA-scope and immunofluorescence analyses (n=3). All n values represent biological replicates.

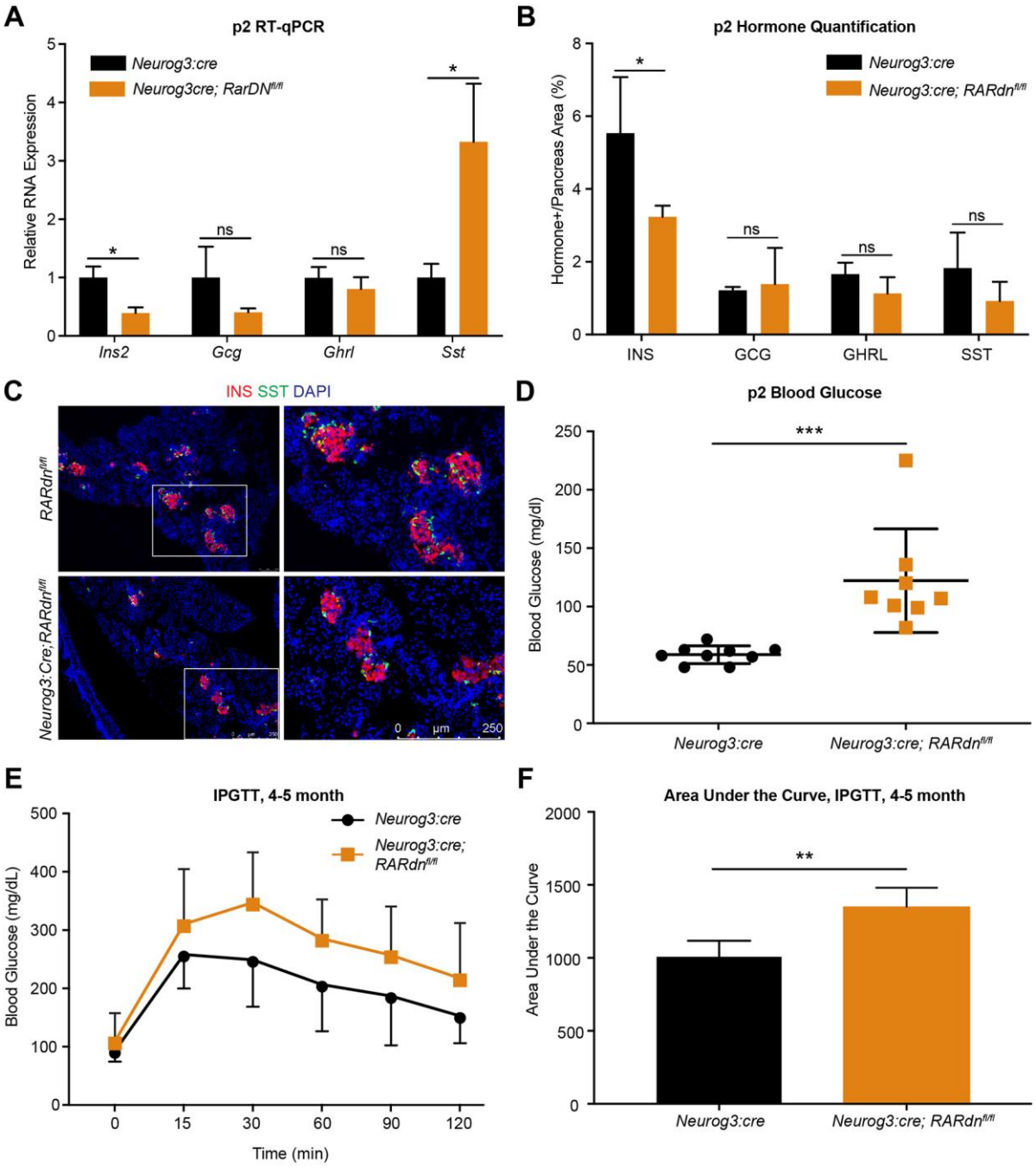

Fig. 2. Postnatal blood glucose homeostasis is disrupted in RA mutants. (A) Gene expression analysis by RT-qPCR of p2 whole pancreata from *RARdn*$^{flox/flox}$*;Neurog3:cre* mutants (n=3, statistical analysis was completed by the Benjamini, Krieger, and Yekutieli two-stage step method to correct for multiple comparisons, q values <0.05* are significant). (B) Quantification of hormones in p2 pancreas (n=5, statistical analysis was completed for multiple t-tests using the Holm-Sidak method to correct for multiple comparisons, padj <0.05* is significant). (C) Representative images of immunofluorescence at p2 for INS and SST. (D) Blood

glucose at p2, reported in mg/dl, statistical analysis was completed by the unpaired, parametric t-test method, p<0.0005*** is significant. (E) Glucose tolerance tests between 4-5 month male *RARdn*$^{fl/fl}$*;Neurog3:cre* mutants (n=4). (F) Area under the curve of IPGTTs in E (statistical analysis was completed by the unpaired, parametric t-test method, p<0.005** is significant). All n values represent biological replicates.

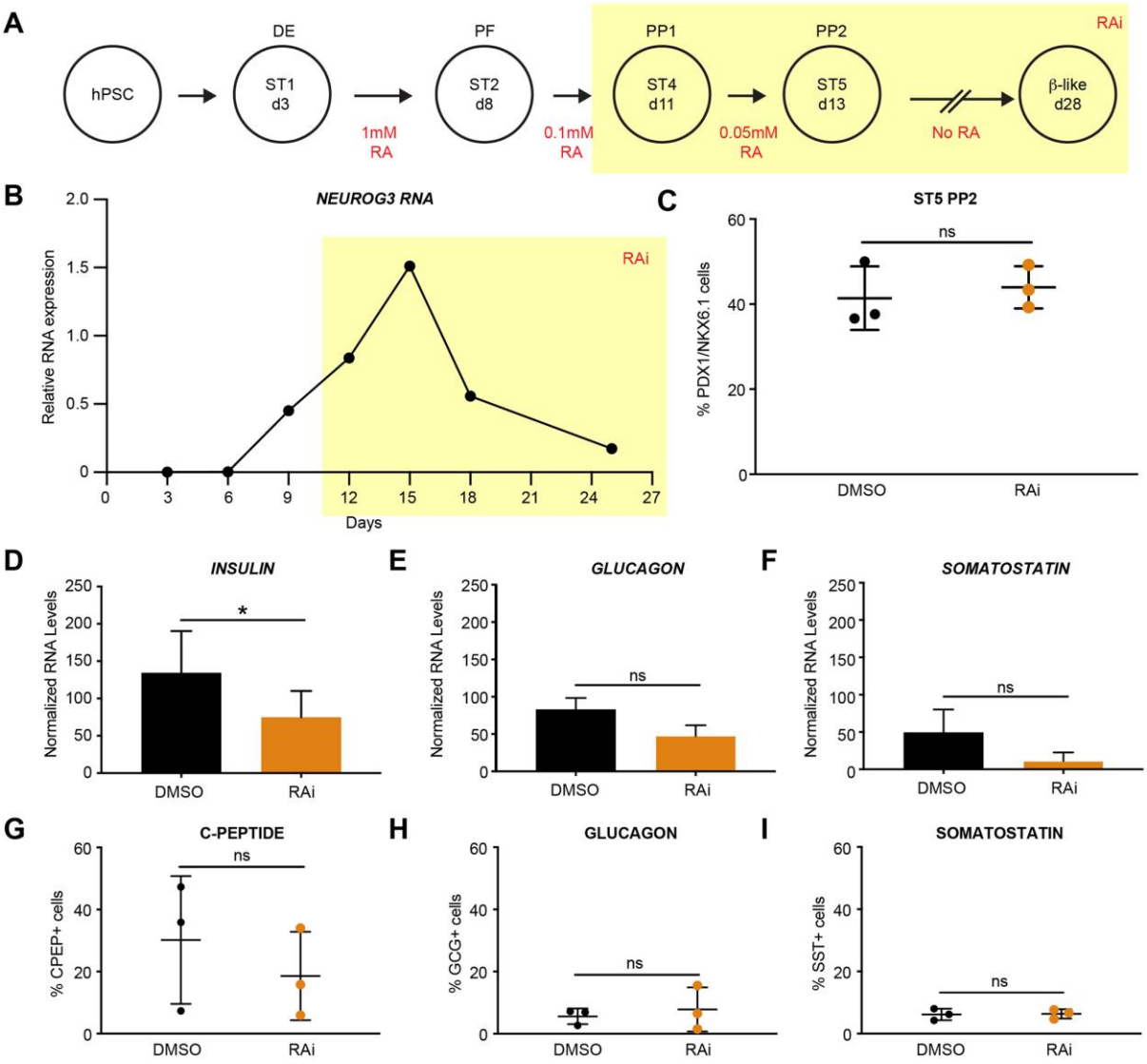

Fig. 3: Human β cell differentiation requires RA signaling after posterior foregut formation. (A) Summary of human β cell differentiations with RA addition in red. Highlighted area indicates when exogenous RA was removed from the media and RA inhibitor (RAi) was added. (B) Gene expression analysis by RT-qPCR of *NEUROG3* expression, normalized to *TBP*. (C) Percentage of PDX1+/NKX6.1+ cells at ST5 of the differentiation with and without RAi treatment (n=3 per treatment, statistical analysis was completed by the unpaired, parametric t-test method, P>0.05 not significant). (D-F) Gene expression analysis by RT-qPCR of *INS*, *GCG*, and *SST* expression at day 28, normalized to *TBP* for total RNA and *CHGB* for endocrine cells to control for differentiation efficiency (n=3 per treatment, statistical analysis was completed by the paired, parametric t-test method, p<0.05* is significant). (G-I) Percentage of cells positive for C-PEPTIDE, GLUCAGON, and SOMATOSTATIN by

flow cytometric analysis (n=3 per treatment, statistical analysis was completed by the unpaired, parametric t-test method, $p>0.05$, not significant). All n values represent biological replicates.

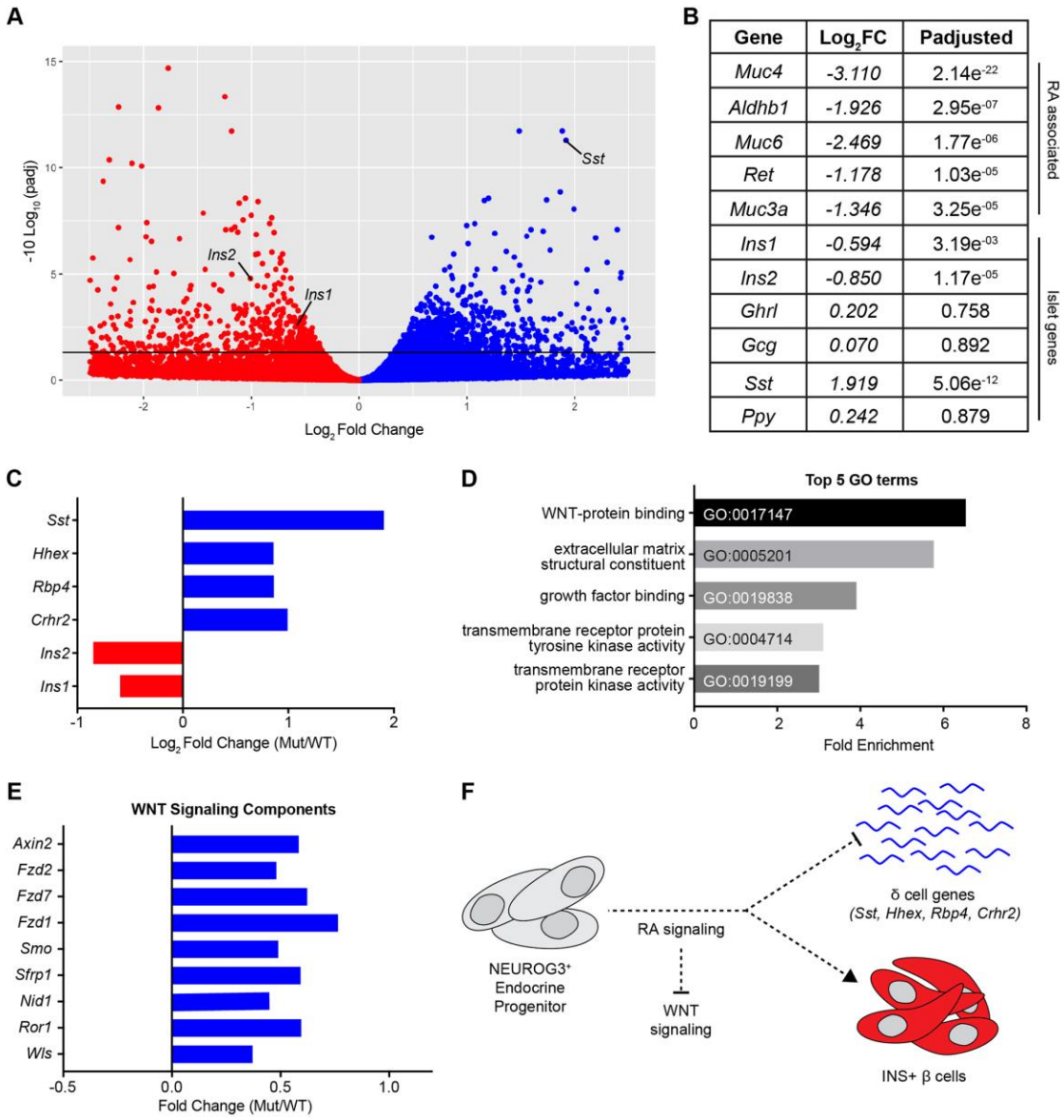

Gene	Log_2FC	Padjusted	
Muc4	*-3.110*	$2.14e^{-22}$	RA associated
Aldhb1	*-1.926*	$2.95e^{-07}$	
Muc6	*-2.469*	$1.77e^{-06}$	
Ret	*-1.178*	$1.03e^{-05}$	
Muc3a	*-1.346*	$3.25e^{-05}$	
Ins1	*-0.594*	$3.19e^{-03}$	Islet genes
Ins2	*-0.850*	$1.17e^{-05}$	
Ghrl	*0.202*	0.758	
Gcg	*0.070*	0.892	
Sst	*1.919*	$5.06e^{-12}$	
Ppy	*0.242*	0.879	

Fig. 4 – RA signaling inhibits the WNT pathway to promote β cell specification and inhibit the δ cell transcriptional program (A) Differentially expressed genes from whole transcriptome analysis by RNA-sequencing in *RARdn$^{flox/flox}$;Neurog3:cre* mutants (n=3). (B) A selection of genes from (A) with Log_2Fold change and P-adjusted value (padj ≤ 0.05 is significant). (C) A selection of upregulated δ cell genes compared to *Ins1/2* (*Crhr2* padj = 0.053) (D) Significantly upregulated GO terms via Panther analysis from genes reported in (A) and Table S1. (E) Significantly enriched WNT signaling components (GO:0017147). (F) Model demonstrating that during endocrine differentiation, RA signaling represses WNT to promote β cell differentiation and repress δ cell genes. All n values represent biological replicates.

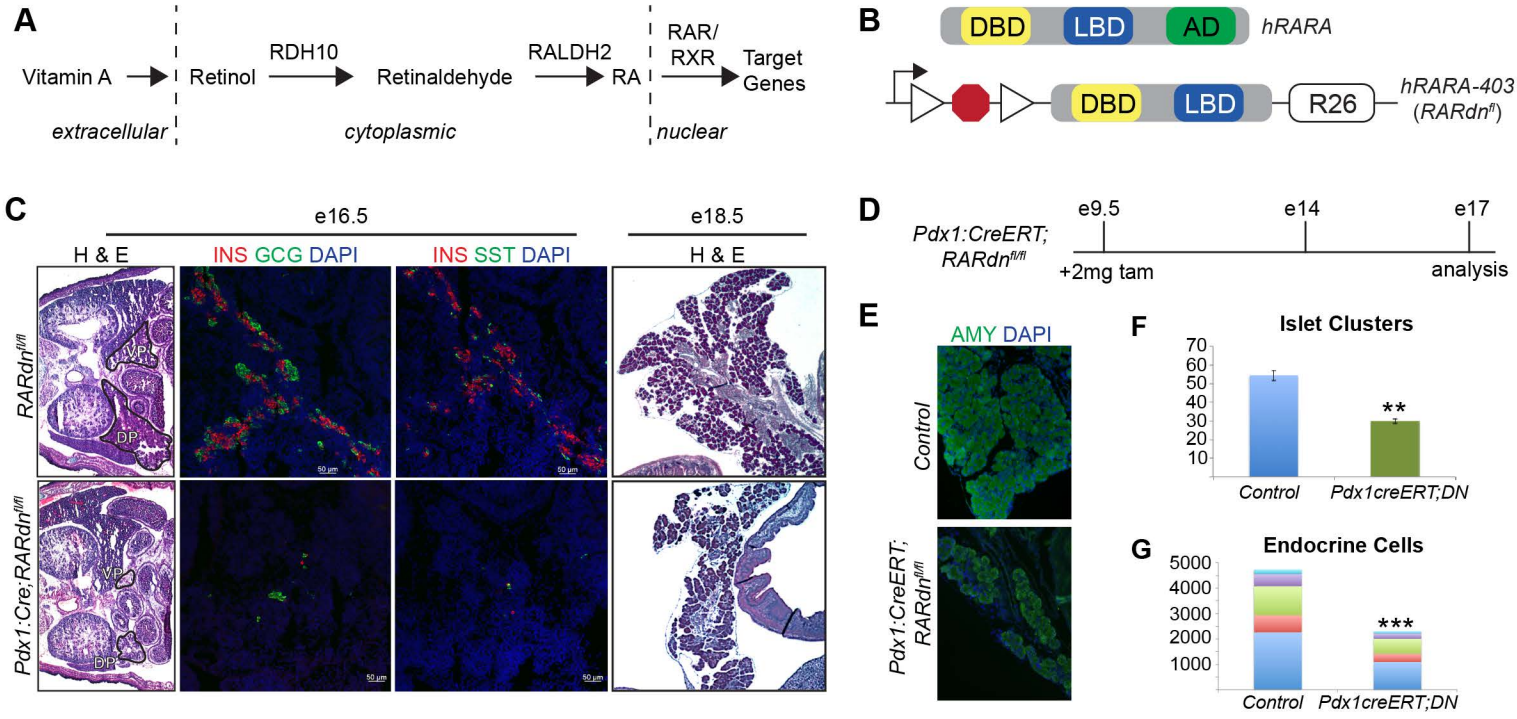

Figure S1. The *RAR* dominant negative efficiently inhibits RA signaling during pancreas development. (A) Summary of the retinoic acid signaling pathway. (B) Diagram of the *RAR* dominant negative (*RARdn*^{flox}), a truncated version human *RARA* gene lacking an activation domain and placed in the *Rosa26* locus. (C) Combined H & E and immunofluorescence analysis of *RARdn*$^{flox/flox}$*; Pdx1:cre* mice examining pancreas morphology and hormone+ endocrine cells at e16.5 and e18.5. DP is dorsal pancreas, VP is ventral pancreas in the H & E (n=3). (D) Summary of tamoxifen injection and analysis schedule of experiments described in S1E-G. (E) Immunofluorescence analysis of *RARdn*$^{flox/flox}$*;Pdx1:creERT* AMYLASE in the pancreas at e17.0. (F-G) Number of islet clusters and endocrine cells, respectively, in tamoxifen treated *RARdn*$^{flox/flox}$*;Pdx1:creERT* pancreata compared to either cre-alone or *RARdn*$^{flox/flox}$ alone controls at e17.0. In G, blue is INS, red is GCG, green is PPY, purple is SST, and light blue is GHRL (n=5).

Table S1 – Differentially expressed genes in e16.5 RA mutants Genes significantly changed in *RARdn*$^{flox/flox}$*; Neurog3:cre* mutants compared to *Neurog3:cre* only controls (padj < 0.05). To filter low reads, all genes with a raw read count of 0 in any one of columns H-M are not reported. DESeq2 was used to generate differentially expressed genes.

Click here to Download Table S1

Table S2 – Binding site identification within significantly differentially expressed genes at e16.5 Putative RARα binding sites within 500bp of the transcriptional start site of each of the genes from Table S1.

Click here to Download Table S2

Table S3 – Antibodies and Probes

Antibody/Probe	Source	Catalog/RRID Number
DAPI (4',6-diamidino-2-phenylindole) (1:1000)	Thermo Fisher	Cat# D1306 RRID:AB_2629482
Rabbit anti-Glucagon (1:250)	Cell Signaling Technologies	Cat# 2760S RRID:AB_659831
Guinea Pig anti-Insulin (1:5)	Dako/Agilent	Cat# IR00261-2
Rabbit anti-Somatostatin (1:500)	Phoenix	Cat# H-060-03 RRID:AB_2687415
Rabbit anti-amylase (1:500)	Sigma	Cat# A8273 RRID: AB_258380
Goat anti-Ghrelin (1:500)	Santa Cruz	Cat# sc-10368, RRID:AB_2232479
Rabbit anti-Ki67 (1:500)	Abcam	Cat# Ab15580 RRID:AB_443209
488 goat anti-guinea pig (1:500)	Thermo Fisher/Invitrogen	Cat# A11073 RRID:AB_2534117
555 goat anti-guinea pig (1:500)	Thermo Fisher/Invitrogen	Cat# A21435 RRID:AB_1500610
488 donkey anti-rabbit (1:500)	Thermo Fisher/Invitrogen	Cat# A21206 RRID:AB_141708
594 donkey ant-rabbit (1:500)	Thermo Fisher/Invitrogen	Cat# A21207 RRID:AB_141637
647 goat anti-rabbit (1:500)	Thermo Fisher/Invitrogen	Cat# A21244 RRID:AB_141663
488 donkey anti-goat (1:500)	Thermo Fisher/Invitrogen	Cat# A11055 RRID:AB_2534102
555 donkey anti-goat (1:500)	Thermo Fisher/Invitrogen	Cat# A21432 RRID:AB_2535853
Biotinylated goat anti PDX-1/IPF1	R&D Systems	Cat# BAF2419 RRID:AB_416757
Mouse IgG1 anti-NKX6.1	DSHB	Cat# F55A10 RRID:AB_532378
Rat anti-Somatostatin	Santa Cruz	Cat# sc-47706 RRID:AB_628268

Mouse IgG1 anti-Glucagon	Sigma-Aldrich	Cat# G2654 RRID:AB_259852
Rabbit anti-C-Peptide	Cell Signaling	Cat# 4593S RRID:AB_10691857
Goat anti-mouse IgG1-488	Jackson Immunoresearch	Cat# 115-545-205 RRID:AB_2338854
Goat anti-mouse IgG1-PE	Jackson Immunoresearch	Cat# 115-115-205 RRID:AB_2338620
Goat anti-mouse IgG1-647	Jackson Immunoresearch	Cat# 115-605-205 RRID:AB_2338916
Goat anti-rabbit Alexa 647	Invitrogen	Cat# A21245 RRID:AB_2535813
Goat anti-rabbit IgG-PE	Jackson Immunoresearch	Cat# 111-116-144 RRID:AB_2337985
Donkey anti-mouse IgG Alexa 647	Jackson Immunoresearch	Cat# 715-605-150 RRID:AB_2340862
Donkey anti-rabbit IgG-PE	Jackson Immunoresearch	Cat# 711-116-152 RRID:AB_2340599
Streptavidin, Pacific Blue conjugate	Thermo Fisher Scientific	Cat# S11222
Goat anti Rat Alexa 647	Thermo Fisher scientific	Cat# A21247 RRID:AB_141778
Mm Ins2-01	ACD Bio	Cat# 497811
Mm Sst C3	ACD Bio	Cat# 404631-C3
Mm Gcg C2	ACD Bio	Cat# 400601-C2
Opal 520 Reagent (1:1500)	Akoya Biosciences	Cat# FP1487A
Opal 570 Reagent (1:1000)	Akoya Biosciences	Cat# FP1488A
Opal 620 Reagent (1:1000)	Akoya Biosciences	Cat# FP1495A
Opal 650 Reagent (1:1000)	Akoya Biosciences	Cat# FP1496A
Taqman Probe Ins1	ThermoFisher	Cat# Mm01950294
Taqman Probe Ins2	ThermoFisher	Cat# Mm00731595
Taqman Probe Gcg	ThermoFisher	Cat# Mm00801714
Taqman Probe Sst	ThermoFisher	Cat# Mm00436671
Taqman Probe Ghrl	ThermoFisher	Cat# Mm00445450
Taqman Probe Actb	ThermoFisher	Cat# Mm00607939

Table S4 – Quantitative real time PCR and genotyping primers

Assay	Animal	Primer Name	Sequence
PCR	Mouse	RARdn_F	ATG GTG TAC ACG TGT CAC C
PCR	Mouse	RARdn_R	CAC CTT CTC AAT GAG CTC C
PCR	Mouse	General Cre_F	CTG CCA CGA CCA AGT GAC AGC
PCR	Mouse	General Cre_R	CTT CTC TAC ACC TGC GGT GCT
PCR	Mouse	Neurog3cre_F	CGT GCA GTG ACC TCT AAG TCA G
PCR	Mouse	Neurog3cre_R	GTG AAA CAG CAT TGC TGT CAC TT
PCR	Mouse	Pdx1cre_F	CTG GAC TAC ATC TTG AGT TGC
PCR	Mouse	Pdx1cre_R	GGT GTA CGG TCA GTA AAT TTG
PCR	Mouse	RosaWT_F	AAG GGA GCT GCA GTG GAG TA
PCR	Mouse	RosaWT_R	CCG AAA ATC TGT GGG AAG TC
PCR	Mouse	Pdx1Cre ER_F	AGC AGT GGA GAA CTG TCA AAG CGA
PCR	Mouse	Pdx1Cre ER_R	TGG ATG TGG TCC TTC TCT TCC AGA
qPCR	Human	INS_F	TTT GTG AAC CAA CAC CTG TGC GG
qPCR	Human	INS_R	GCG GGT CTT GGG TGT GTA GAA GAA
qPCR	Human	GCG_F	TTC CCA GAA GAG GTC GCC ATT GTT
qPCR	Human	GCG_R	CAA CCA GTT TAT AAA GTC CCT GGC GG
qPCR	Human	SST_F	GAG AAT GAT GCC CTG GAA CCT GAA GA
qPCR	Human	SST_R	ATT CTT GCA GCC AGC TTT GCG T
qPCR	Human	TBP_F	TTG CTG AGA AGA GTG TGC TGG AGA TG
qPCR	Human	TBP_R	CGT AAG GTG GCA GGC TGT TGT T
qPCR	Human	CHGB_F	TTG CTG AGA AGA GTG TGC TGG AGA TG
qPCR	Human	CHGB_R	CGT AAG GTG GCA GGC TGT TGT T

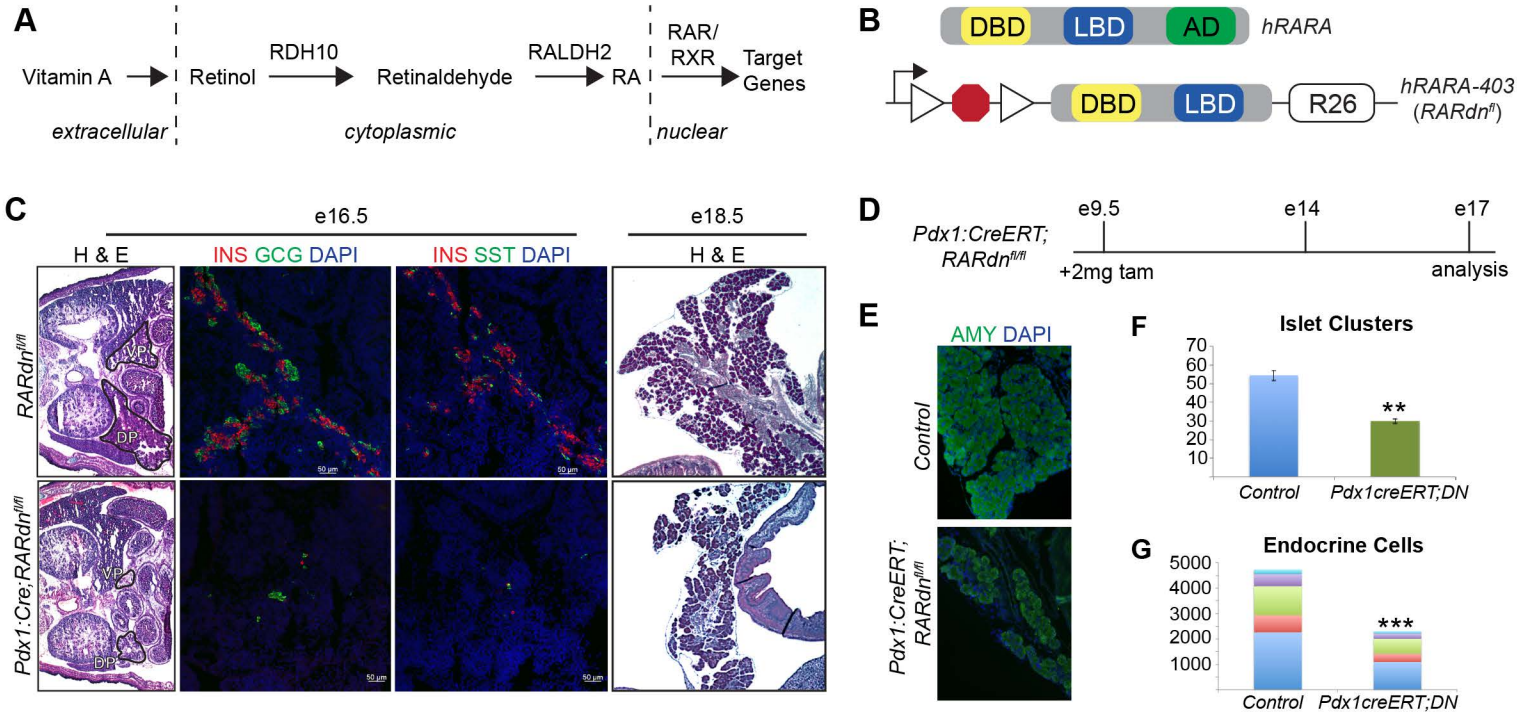

Figure S1. The *RAR* dominant negative efficiently inhibits RA signaling during pancreas development. (A) Summary of the retinoic acid signaling pathway. (B) Diagram of the *RAR* dominant negative (*RARdn*^{flox}), a truncated version human *RARA* gene lacking an activation domain and placed in the *Rosa26* locus. (C) Combined H & E and immunofluorescence analysis of *RARdn*$^{flox/flox}$*; Pdx1:cre* mice examining pancreas morphology and hormone+ endocrine cells at e16.5 and e18.5. DP is dorsal pancreas, VP is ventral pancreas in the H & E (n=3). (D) Summary of tamoxifen injection and analysis schedule of experiments described in S1E-G. (E) Immunofluorescence analysis of *RARdn*$^{flox/flox}$*;Pdx1:creERT* AMYLASE in the pancreas at e17.0. (F-G) Number of islet clusters and endocrine cells, respectively, in tamoxifen treated *RARdn*$^{flox/flox}$*;Pdx1:creERT* pancreata compared to either cre-alone or *RARdn*$^{flox/flox}$ alone controls at e17.0. In G, blue is INS, red is GCG, green is PPY, purple is SST, and light blue is GHRL (n=5).

Table S1 – Differentially expressed genes in e16.5 RA mutants Genes significantly changed in *RARdn*$^{flox/flox}$*; Neurog3:cre* mutants compared to *Neurog3:cre* only controls (padj < 0.05). To filter low reads, all genes with a raw read count of 0 in any one of columns H-M are not reported. DESeq2 was used to generate differentially expressed genes.

Click here to Download Table S1

Table S2 – Binding site identification within significantly differentially expressed genes at e16.5 Putative RARα binding sites within 500bp of the transcriptional start site of each of the genes from Table S1.

Click here to Download Table S2

Table S3 – Antibodies and Probes

Antibody	SOURCE	IDENTIFIER
DAPI (4',6-diamidino-2-phenylindole) (1:1000)	Thermo Fisher	Cat# D1306 RRID:AB_2629482
Rabbit anti-Glucagon (1:250)	Cell Signaling Technologies	Cat# 2760S RRID:AB_659831
Guinea Pig anti-Insulin (1:5)	Dako/Agilent	Cat# IR00261-2
Rabbit anti-Somatostatin (1:500)	Phoenix	Cat# H-060-03 RRID:AB_2687415
Rabbit anti-amylase (1:500)	Sigma	Cat# A8273 RRID: AB_258380
Goat anti-Ghrelin (1:500)	Santa Cruz	Cat# sc-10368, RRID:AB_2232479
Rabbit anti-Ki67 (1:500)	Abcam	Cat# Ab15580 RRID:AB_443209
488 goat anti-guinea pig (1:500)	Thermo Fisher/Invitrogen	Cat# A11073 RRID:AB_2534117
555 goat anti-guinea pig (1:500)	Thermo Fisher/Invitrogen	Cat# A21435 RRID:AB_1500610
488 donkey anti-rabbit (1:500)	Thermo Fisher/Invitrogen	Cat# A21206 RRID:AB_141708
594 donkey ant-rabbit (1:500)	Thermo Fisher/Invitrogen	Cat# A21207 RRID:AB_141637
647 goat anti-rabbit (1:500)	Thermo Fisher/Invitrogen	Cat# A21244 RRID:AB_141663
488 donkey anti-goat (1:500)	Thermo Fisher/Invitrogen	Cat# A11055 RRID:AB_2534102
555 donkey anti-goat (1:500)	Thermo Fisher/Invitrogen	Cat# A21432 RRID:AB_2535853
Biotinylated goat anti PDX-1/IPF1 (1:50)	R&D Systems	Cat# BAF2419 RRID:AB_416757
Mouse IgG1 anti-NKX6.1(1:250)	DSHB	Cat# F55A10 RRID:AB_532378
Rat anti-Somatostatin (1:100)	Santa Cruz	Cat# sc-47706 RRID:AB_628268
Mouse IgG1 anti-Glucagon (1:2000)	Sigma-Aldrich	Cat# G2654 RRID:AB_259852
Rabbit anti-C-Peptide (1:100)	Cell Signaling	Cat# 4593S RRID:AB_10691857
Goat anti-mouse IgG1-488 (1:400)	Jackson Immunoresearch	Cat# 115-545-205 RRID:AB_2338854
Goat anti-mouse IgG1-PE (1:400)	Jackson Immunoresearch	Cat# 115-115-205 RRID:AB_2338620
Goat anti-mouse IgG1-647 (1:400)	Jackson Immunoresearch	Cat# 115-605-205 RRID:AB_2338916
Goat anti-rabbit alexa 647 (1:400)	Invitrogen	Cat# A21245 RRID:AB_2535813
Goat anti-rabbit IgG-PE (1:400)	Jackson Immunoresearch	Cat# 111-116-144 RRID:AB_2337985
Donkey anti-mouse IgG alexa647 (1:400)	Jackson Immunoresearch	Cat# 715-605-150 RRID:AB_2340862
Donkey anti-rabbit IgG-PE (1:400)	Jackson Immunoresearch	Cat# 711-116-152 RRID:AB_2340599

Streptavidin, Pacific Blue conjugate (1:400)	Thermo Fisher Scientific	Cat# S11222
Goat anti Rat alexa 647 (1:400)	Thermo Fisher scientific	Cat# A21247 RRID:AB_141778
Mm Ins2-01 (pre-diluted)	ACD Bio	Cat# 497811
Mm Sst C3 (1:150)	ACD Bio	Cat# 404631-C3
Mm Gcg C2 (1:150)	ACD Bio	Cat# 400601-C2
Opal 520 Reagent (1:1500)	Akoya Biosciences	Cat# FP1487A
Opal 570 Reagent (1:1000)	Akoya Biosciences	Cat# FP1488A
Opal 620 Reagent (1:1000)	Akoya Biosciences	Cat# FP1495A
Opal 650 Reagent (1:1000)	Akoya Biosciences	Cat# FP1496A
Taqman Probe Ins1	ThermoFisher	Cat# Mm01950294
Taqman Probe Ins2	ThermoFisher	Cat# Mm00731595
Taqman Probe Gcg	ThermoFisher	Cat# Mm00801714
Taqman Probe Sst	ThermoFisher	Cat# Mm00436671
Taqman Probe Ghrl	ThermoFisher	Cat# Mm00445450
Taqman Probe Actb	ThermoFisher	Cat# Mm00607939

Table S4 – Quantitative real time PCR and genotyping primers

Assay	Animal	Primer Name	Sequence
PCR	Mouse	RARdn_F	ATG GTG TAC ACG TGT CAC C
PCR	Mouse	RARdn_R	CAC CTT CTC AAT GAG CTC C
PCR	Mouse	General Cre_F	CTG CCA CGA CCA AGT GAC AGC
PCR	Mouse	General Cre_R	CTT CTC TAC ACC TGC GGT GCT
PCR	Mouse	Neurog3cre_F	CGT GCA GTG ACC TCT AAG TCA G
PCR	Mouse	Neurog3cre_R	GTG AAA CAG CAT TGC TGT CAC TT
PCR	Mouse	Pdx1cre_F	CTG GAC TAC ATC TTG AGT TGC
PCR	Mouse	Pdx1cre_R	GGT GTA CGG TCA GTA AAT TTG
PCR	Mouse	RosaWT_F	AAG GGA GCT GCA GTG GAG TA
PCR	Mouse	RosaWT_R	CCG AAA ATC TGT GGG AAG TC
PCR	Mouse	Pdx1Cre ER_F	AGC AGT GGA GAA CTG TCA AAG CGA
PCR	Mouse	Pdx1Cre ER_R	TGG ATG TGG TCC TTC TCT TCC AGA
qPCR	Human	INS_F	TTT GTG AAC CAA CAC CTG TGC GG
qPCR	Human	INS_R	GCG GGT CTT GGG TGT GTA GAA GAA
qPCR	Human	GCG_F	TTC CCA GAA GAG GTC GCC ATT GTT
qPCR	Human	GCG_R	CAA CCA GTT TAT AAA GTC CCT GGC GG
qPCR	Human	SST_F	GAG AAT GAT GCC CTG GAA CCT GAA GA
qPCR	Human	SST_R	ATT CTT GCA GCC AGC TTT GCG T
qPCR	Human	TBP_F	TTG CTG AGA AGA GTG TGC TGG AGA TG
qPCR	Human	TBP_R	CGT AAG GTG GCA GGC TGT TGT T
qPCR	Human	CHGB_F	TTG CTG AGA AGA GTG TGC TGG AGA TG
qPCR	Human	CHGB_R	CGT AAG GTG GCA GGC TGT TGT T